

Transverse initiation of an insensitive explosive in a layered slab geometry: initiation modes

E K Anderson, T D Aslam and S I Jackson

Shock and Detonation Physics Group, WX-9, LANL, Los Alamos, NM 87545

E-mail: eanderson@lanl.gov

Abstract. Experiments are presented that explore the shock initiating layer dynamics in an insensitive high explosive. Tests were conducted with a PBX 9502 (95% TATB, 5% Kel-F 800) slab bonded on one side to a PBX 9501 (95% HMX, 2.5% Estane, 2.5% BDNPAF) slab. For each test, a planar detonation in the PBX 9501 was generated to drive a shock intended to initiate the PBX 9502. Shocks of sufficient strength generated a region of delayed reaction in the PBX 9502 immediately adjacent to the PBX9501. Slow reactions in this region coupled energy with the initial shock resulting in a transition to detonation further from the 9501/9502 interface, a process analogous to the run-up to detonation in shocked one-dimensional (1D) explosive configurations. The thickness of the PBX 9501 layer was varied to control the strength and duration of the transmitted shock. Phase velocities at the explosive outer surfaces and wave-front breakout shapes are reported and discussed.

1. Introduction

Shocks of sufficient strength can generate hot spots in a heterogeneous explosive either from shock reflection and refraction around the explosive particles, or heating from the collapse of voids. These hotspots release chemical energy which can couple with the primary shock and drive a transition to detonation [1]. Both wedge tests and gas gun experiments have been used to characterize this phenomenon in 1D geometries.

A phenomenon analogous to the 1D run-up and transition to detonation in wedge tests and gas gun experiments occurs in two-dimensions in geometries where one explosive slab is placed next to a slab of a different explosive. Detonation in the faster explosive can drive a transverse shock in the slower explosive. In the region immediately adjacent to the faster explosive, which we will refer to as the initiating layer, this transverse shock is not a detonation. However, further from the interface, the transverse shock, strengthened by slow reactions and heat release in the initiating layer, transitions to full detonation.

In the presently reported series of tests, the behavior of PBX 9502 slabs bonded to PBX 9501 slabs along a common face is investigated. PBX 9501 is more sensitive than PBX 9502, and displays a higher detonation velocity [2]. Hill et al. [3] have investigated assemblies consisting of 130 mm x 150 mm x 8 mm PBX 9502 bonded to 130 mm x 150 mm x 3 mm thick PBX 9501, but assemblies with PBX 9501 slabs of thickness less than 3.0 mm have not been previously studied. In the present work, we vary the thickness of the PBX 9501 layer from 2.5 mm down to 0.5 mm in order to drive shocks of decreasing strength transversely into the PBX 9502 slab. By studying these assemblies, the following goals can be met:



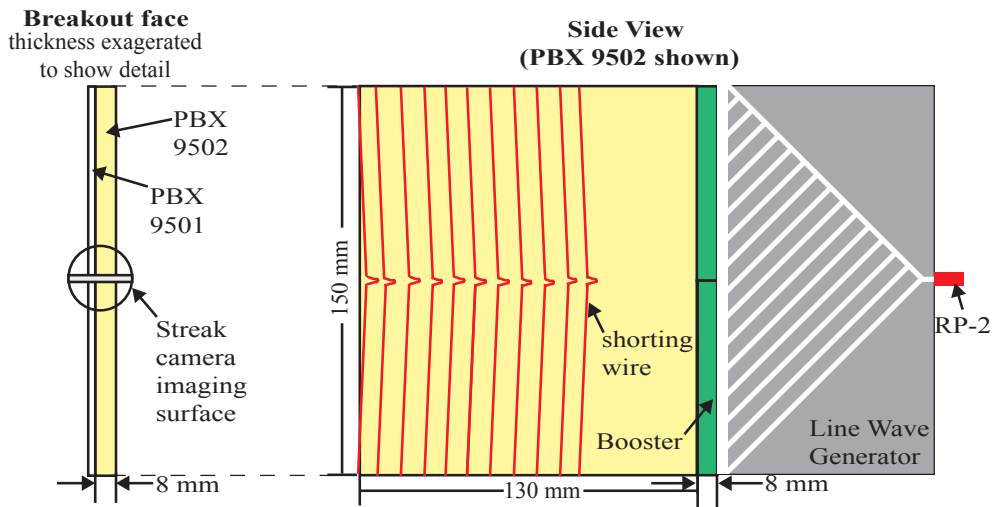


Figure 1. Diagram of explosive assembly showing key dimensions.

- (i) Determine how the initiating layer thickness varies with driver strength (PBX 9501 thickness).
- (ii) Identify the limiting value where the PBX 9501 will not initiate the PBX 9502.

2. Shot Assembly

The dimensions and densities of the explosive slabs tested are listed in table 1. The densities of the PBX 9502 slabs were 0.9-1.2% below the normally specified value of 1.890 g/cm³. The tested PBX 9501 slab densities were within 0.2% of the specified density of 1.836 g/cm³.

Table 1. Measured dimensions in mm and densities in g/cm³ of assemblies tested. Length and width measured for PBX 9502 slab. * indicates nominal value.

Length	Width	PBX 9502 Thickness	PBX 9502 Density	PBX 9501 Thickness	PBX9501 Density
149.96	130.02	8.00	1.8719	0.56	1.8354
150.02	129.99	8.00	1.8697	1.14	1.8346
149.96	130.07	8.00	1.8722	1.55	1.8355
150.00	130.00	8.00	1.8704	2.00	1.8327
150.01	130.02	8*	1.8675	2.5*	1.8342

Figure 1 shows the assembly geometry. The initiating shock train consisted of a RP-2 detonator (mfg. by Teledyne RISI Inc.), line wave generator, and an 8 mm x 8 mm x 150 mm Composition B booster bonded to one 150 mm edge of the slab assembly. For each assembly, the PBX 9501 was bonded to the PBX 9502 using Angstrom Bond AB9320. Eleven evenly spaced shorting wires were taped to each exposed 150 mm x 130 mm face, starting 30 mm from the booster. These wires are visible in the side view of figure 1 for the PBX 9502 face. The streak camera imaging surface is visible in the breakout face view.

3. Results and Analysis

3.1. Shorting Wires

Shorting wires on both sides of the explosive assemblies were placed approximately every 9 mm starting after a 30 mm run distance from the Comp B booster. The positions of the shorting wires were recorded to within $\pm 0.5 \mu\text{m}$ using a binocular microscope equipped with a 3-axis translation stage. The resulting spatial data were combined with temporal data recorded on an oscilloscope sampling at 5 GS/s with 1 GHz bandwidth. For each side of the explosive assemblies, a linear fit to the shorting wire time-position data was computed, and the slope was extracted as the phase velocity.

Table 2 displays the shorting wire results from all five assemblies. For the assemblies with 1.5, 2.0, and 2.5-mm-thick PBX 9501 layers, linear fits were obtained with standard errors less than $0.006 \text{ mm}/\mu\text{s}$, which is below 0.1% of the reported velocities. The low standard errors indicate that for these shots, steady detonation waves were observed. The phase velocities on the PBX 9501 side decreased slightly with decreasing PBX 9501 layer thickness. For these shots, the phase velocity measured on the PBX 9502 side was approximately 0.1% slower than on the PBX 9501 side. For the assembly with the 0.5-mm-thick PBX 9501 layer, the phase velocities were substantially lower, at $7.496 \text{ mm}/\mu\text{s}$ on the PBX 9501 side and approximately 0.4% lower on the PBX 9502 side. The decrease in velocities for this shot were expected due to the thickness effect in the PBX 9501 slab. The standard error was quite low for the PBX 9502 side, indicating a steady wave, but higher on the PBX 9501 side, indicating a slightly less steady wave.

The results for the assembly with the 1.0-mm-thick PBX 9501 layer are particularly interesting. The phase velocity on the PBX 9501 side of the assembly was steady and relatively fast at $8.441 \text{ mm}/\mu\text{s}$, but on the PBX 9502 side the phase velocity was nearly $1.0 \text{ mm}/\mu\text{s}$ slower and approximately $0.1 \text{ mm}/\mu\text{s}$ slower at the breakout end of the shot than at the first shorting wire. From the phase velocities, it appears that at this thickness the transverse shock from the PBX 9501 layer was not sufficiently strong to drive a shock in PBX 9502 at velocities near the PBX 9501 detonation velocity. The variation in PBX 9502 phase velocity from one end of the shot to the other indicate that steady shock velocities were not reached by the end of the explosive. High speed video shows that for this shot, a detonation was initiated and consumed slightly more than 50% of the PBX 9502 slab, but failed in the last 40 mm of the explosive as the shock from the adjacent PBX 9501 pushed the PBX 9502 away with insufficient strength to support detonation.

Table 2. Phase velocities measured with shorting wires.

PBX 9501 Thickness (mm)	PBX 9501 Phase Velocity (mm/ μs)	Standard Error (mm/ μs)	PBX 9502 Phase Velocity (mm/ μs)	Standard Error (mm/ μs)
0.5	7.496	0.0410	7.470	0.0022
1.0	8.441	0.0020	7.500-7.620	0.1300
1.5	8.638	0.0018	8.623	0.0045
2.0	8.696	0.0006	8.690	0.0024
2.5	8.731	0.0012	8.723	0.0058

3.2. Streak Camera

For each shot, two still images were recorded with a Cordin 132 streak camera prior to detonation and recording the streak image. Film from the camera was digitized using a scanner set to 6400 DPI resolution. The vertical direction of the streak camera film represents time, not distance, and was converted to a time-scale using the image write speed associated with the streak camera. Next, the phase velocity measured with the shorting wires was used to convert from time to distance in the vertical direction on the film. The result was a separate pixel-mm relationship for both the horizontal and vertical directions on film, that yielded the shape of the wave at breakout from the explosive. Manually selected points along the shock fronts were used to compute linear fits in the detonating and initiating regions. The slope of the linear fit was used to determine the shock angle. The normal velocity was then computed as phase velocity times the cosine of the shock angle.

For each of the five assemblies, linear fits were computed for each point along the shock front using the neighboring points. The window size for computation of these linear fits was varied from 0.16 mm to 0.8 mm in steps of 0.16 mm. Example results of this fitting process are shown for the case of the 1.5-mm-thick PBX 9501 assembly in figure 2. The results of figure 2 are characteristic of the shots with the 1.5-2.5 mm thick PBX 9501 layers, with a clearly visible initiating layer and detonating layer. The initiating layer is visible on the left, with non-linearity apparent in the initiating layer front shape as changing slope and hence normal velocity. Normal velocities in the initiating layer varied from 5.8 to 6.5 mm/ μ s. The window sizes of 0.16 to 0.8 mm are large compared to the size of the initiating layer, leading to some of the variation in normal velocity results seen in the figures.

The transition from initiating layer to detonating PBX 9502 is seen in figure 2 as a large increase in normal velocity over a short distance. The analysis used herein to determine the location of the initiating layer-detonating PBX 9502 transition involved finding the maximum slope of the normal velocity curves. The transition point is displayed on the figure as a vertical line for each window size. Due to the short distance over which the shock transitioned from initiating layer to detonating PBX 9502, the smallest window (0.16 mm) for the linear fits was used for determination of the transition point.

The normal velocity was nearly constant over a region indicated on the figures by black horizontal lines, except for noise of magnitude inversely related to linear fit window size. The horizontal line indicates the region over which the detonating normal velocity was computed.

Initiating layer thickness and normal velocity data is shown for each explosive assembly in table 3. The second column shows the normal velocity for the detonating region in the PBX 9502, and for the assemblies with PBX 9501 layers of 1.5 - 2.5-mm thickness, were approximately 7.5 mm/ μ s. For these cases the initiating layer normal velocities were over 1.0 mm/ μ s slower, and the initiating layers were approximately 1.0 mm thick and decreased with increasing PBX 9501 layer thickness. The assembly with the 0.5-mm-thick PBX 9501 layer displayed no initiating layer. Instead, both explosive layers were initiated by the Composition B booster and both detonated at approximately the same speed due to thickness effects in both explosives causing the detonation velocities to converge. In this case, the PBX 9502 detonation front showed slight curvature, resulting in a normal velocity varying from 7.0-7.5 mm/ μ s depending on the distance from the PBX 9501 slab. For the case of the 1.0-mm-thick PBX 9501 assembly, the entire PBX 9502 slab behaved as initiating layer. The normal velocities were approximately 1.0-2.0 mm/ μ s slower than those observed in the assemblies with thicker PBX 9501 layers. In this case a steady wave profile was not established within the 130 mm length of the explosive assembly.

4. Summary and Conclusions

Explosive assemblies consisting of an 8.0-mm-thick PBX 9502 slab bonded to a PBX 9501 slab ranging from 0.5 to 2.5-mm-thick were tested experimentally. Each assembly was instrumented

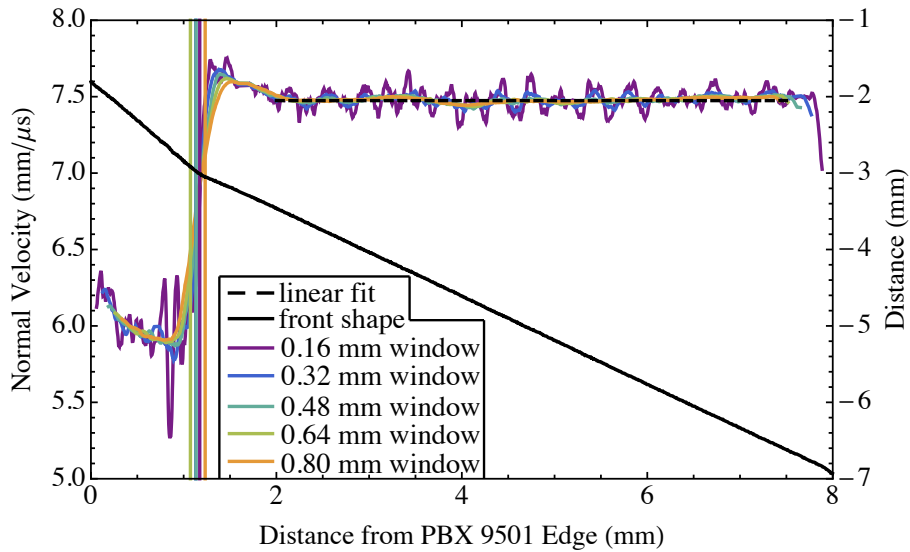


Figure 2. Normal velocity (colors) and front shape (black) in PBX 9502 as a function of distance from PBX 9501 interface (on left) for the 1.5-mm-thick PBX 9501 assembly. Linear fit used to extract normal velocity and vertical lines indicating transition from initiating layer to detonation also shown (black,dashed).

Table 3. Streak camera results for 1.5, 2.0, and 2.5 mm PBX 9501 assemblies.

PBX 9501 Thickness mm	PBX 9502 Normal Velocity mm/μs	Std. Error mm/μs	Initiating Layer Normal Velocity mm/μs	Std. Error mm/μs	Initiating Layer Thickness mm
0.5	7.15-7.47	0.002	none	none	none
1.0	none	none	4.11-5.06	0.080	>8
1.5	7.47	0.004	5.95	0.004	1.17
2.0	7.48	0.002	6.37	0.005	1.05
2.5	7.53	0.005	6.31	0.005	0.80

with ionization wires to measure phase velocities, and detonation breakout was imaged with a streak camera. By decreasing the thickness of the PBX 9501 layer, the strength of the shock driven into the PBX 9502 slab was also decreased. This had the effect of increasing the initiating layer thickness, or shock-to-detonation distance in the transverse direction. The detonation velocity in the PBX 9501 layer was also affected by its thickness, and for the smallest assembly tested, the detonation velocity in the PBX 9501 slab matched that of the PBX 9502 slab.

The experimental results from shorting wires are summarized in table 2, and results from the streak camera are summarized in table 3. Based on these measurements, the results fall into three distinct steady wave configurations based on the thickness of the driving HE:

- (i) *Fast HE initiates slow HE.* Here, similar phase velocities are observed for both PBX 9501 and PBX 9502, with the phase velocity being dictated by the PBX 9501. For this configuration, both an initiating layer and a detonating layer were observed in the PBX

9502. The normal velocity in the detonating PBX 9502 appears to be close to the 1D CJ detonation velocity. This flow regime was displayed by the assemblies with PBX 9501 layers of 1.5, 2.0, and 2.5-mm-thickness. This flow regime was also observed for prior 3.0 mm thick PBX 9501 experiments as well [3].

- (ii) *Fast HE fails to initiate slow HE.* The case of the 1.0 mm PBX 9501 layer demonstrates a boundary between the two steady wave configurations of (i) and (iii). For this case, a steady shock front was observed in the PBX 9501, but not in the PBX 9502 within the 130 mm length of the explosive. One would need thicker than 8mm to transit to detonation, if it would transit to detonation at all.
- (iii) *Coupled fast and slow HE detonation.* This flow regime was displayed by the assembly with the 0.5 mm PBX 9501 slab. For this assembly, the PBX 9501 and PBX 9502 were both initiated by the Composition B booster and detonated at nearly equal velocities. This assembly, and likely even thinner slabs of PBX 9501, represent the case where the PBX 9501 cannot naturally detonate faster than the PBX 9502, thus the detonation structure is likely a function of the composite HE assembly.

Acknowledgments

This effort was funded by the Department of Energy. The test assistance provided by Sam Vincent and Tim Tucker was essential to the completion of this work.

References

- [1] Zhang J, Jackson T, Buckmaster J and Freund J 2012 *Combust. Flame* **159** 1769–1778
- [2] Gibbs T R and Popolato A (eds) 1980 *LASL Explosive Property Data* Los Alamos Series on Dynamic Material Properties (Berkeley, CA: University of California Press)
- [3] Hill L 2013 Double-HE-layer detonation-confinement sandwich tests: The effect of slow-layer density *Manuscript submitted for publication.*